

RADIAL BASIS FUNCTION NETWORK AIDED WIDE-BAND BEAMFORMING FOR DISPERSIVE FADING ENVIRONMENTS

A. Wolfgang, S. Chen, L. Hanzo

School of ECS Univ. of Southampton, SO17 1BJ, UK.
 Tel: +44-23-80-593 125, Fax: +44-23-80-594 508
 {aw03r, sqc, lh}@ecs.soton.ac.uk
 http://www-mobile.ecs.soton.ac.uk

ABSTRACT

A novel Radial Basis Function Network (RBFN) assisted Decision-Feedback aided Space-Time Equalizer (DF-STE) designed for receivers employing multiple antennas is introduced. The proposed receiver structure outperforms the linear Minimum Mean-Squared Error benchmarker and it is less sensitive to both error propagation and channel estimation errors.

1. INTRODUCTION

The capability of receivers employing multiple antennas to increase the achievable system capacity and to suppress the effects of co-channel interference has motivated intense research in the field of space-time equalization [1]. Most contributions however focus on sub-optimal linear receivers or investigate the performance of Maximum-Likelihood Sequence Estimators (MLSE), which suffer from an exponentially increasing complexity as a function of the delay-spread encountered. Owing to encountering non-minimum phase channels the received signal constellation may become linearly non-separable and in order to counteract this problem we introduce a novel non-linear Radial Basis Function Network (RBFN) [2] assisted Space-Time Equalizer (STE) for uplink communication scenarios. For the sake of complexity reduction an RBF-aided decision feedback (DF) structure is used, which necessitates the detection of all users. The investigated scenario assumes the presence of multiple users communicating with the Base-Station (BS) over Single-Input Multiple-Output (SIMO) correlated Rayleigh fading channels, which are generated employing a procedure based on the Third Generation Partnership Project's (3GPP) Spatial Channel Model (SCM) [3].

2. SYSTEM MODEL

The system considered consists of Q number of Binary Phase Shift Keying (BPSK) modulated sources and a BS receiver, which is assumed to employ L antennas. The channel output signal of the l^{th} antenna element at time instant t

can then be written as

$$x_l(t) = \sum_{q=1}^Q \sum_{k=0}^K h_{lq,k} s_q(t-k) + \eta(t), \quad (1)$$

where $h_{lq,k}$ is the complex valued channel gain of the k^{th} multi-path component describing the channel between the q^{th} source and the l^{th} receiver antenna, K is the number of multi-path components and $\eta(t)$ is the complex valued Additive White Gaussian Noise (AWGN) having a variance of $E[|\eta_l(t)|^2] = 2\sigma^2$. Each of the receiver's antenna elements is followed by a tapped delay line of length m , which is also referred to as the feed-forward section of the RBF-aided STE as shown in Figure 1. In vectorial notation, the channel output can be expressed by the super-vector $\mathbf{x}(t) = [\mathbf{x}(t)^T, \dots, \mathbf{x}(t-m+1)^T]^T$, where $\mathbf{x}(t)$ is a column vector hosting the L number of antenna-element output signals $x_l(k)$ given in (1). The relation between the signal transmitted by the Q sources and the channel output for channel tap k is described by a $(L \times Q)$ -dimensional matrix \mathbf{H}_k where the $(lq)^{th}$ element of the matrix is given as $h_{lq,k}$. The super-matrix \mathbf{H} representing the total system can then be obtained by concatenating the $(L \times Q)$ -dimensional matrices \mathbf{H}_k , yielding:

$$\mathbf{H} = \begin{pmatrix} \mathbf{H}_k & \cdots & \mathbf{H}_{k-m+1} & 0 & \cdots & 0 \\ & & \ddots & & \ddots & \\ 0 & \cdots & 0 & \mathbf{H}_k & \cdots & \mathbf{H}_{k-m+1} \end{pmatrix}.$$

The channel output vector $\mathbf{x}(t)$ can now be expressed as

$$\begin{aligned} \mathbf{x}(t) &= \mathbf{H} [\mathbf{s}(t)^T, \dots, \mathbf{s}(t-m+1)^T]^T \\ &+ [\boldsymbol{\eta}_1(t)^T, \dots, \boldsymbol{\eta}_L(t)^T]^T \\ &= \mathbf{H}\mathbf{s}(t) + \boldsymbol{\eta}(t) \\ &= \bar{\mathbf{x}}(t) + \boldsymbol{\eta}(t), \end{aligned} \quad (2)$$

where $\mathbf{s}(t) = [s_1(t), \dots, s_Q(t)]^T$ is a column vector containing the symbols transmitted by the Q sources and $\boldsymbol{\eta}_l(t) = [\eta_l(t), \dots, \eta_l(t-m+1)]^T$. Assuming that all sources transmit with identical power, the Signal to Noise

The financial support of the EU under the auspices of the Phoenix project is gratefully acknowledged. The authors are also grateful to their colleagues for the enlightenment gained within the Phoenix consortium.

Ratio (SNR) of user q is given as

$$\text{SNR}_q = \frac{\sum_{l=1}^L \sum_{k=0}^K E[|h_{lq,k}|^2]}{2\sigma^2}. \quad (3)$$

3. RECEIVER

The proposed receiver structure consists of two parts, namely the RBFN assisted DF-STE and a Kalman filter based channel estimator. The RBFN parameters may be estimated directly but this approach has the drawback that it requires a long training period and has a poor tracking performance. By contrast, the cost function that is more straightforward to minimize for the channel estimator is the MMSE and the RBFN may be constructed based on the MMSE-optimized channel estimator, as it will be shown in the next sub-section.

3.1. DF-STE

The performance of both linear and non-linear equalizers can be enhanced by incorporating a decision feedback structure in the receiver [2], as shown in Figure 1. In addition to the feed-forward section, the DF-STE is then characterized by the decision delay Δ and the decision feedback order n . Note that the oldest symbol vector, which still influences the detected symbol $\hat{s}_q(t-\Delta)$ is $s(t-m+1-K)$. Furthermore, the oldest feedback symbol vector is $s(k-\Delta-n)$. Without loss of generality we therefore chose $n = m+K-1-\Delta$ for the derivation of the proposed DF-STE. In order to describe the feedback structure, we first divide the system matrix \mathbf{H} into two sub-matrices $\mathbf{H} = [\mathbf{H}_1 \mathbf{H}_2]$, where \mathbf{H}_1 hosts the first $Q(\Delta+1)$ columns of \mathbf{H} and \mathbf{H}_2 represents the last Qn columns in \mathbf{H} . The array output can then be written as

$$\mathbf{x}(t) = \mathbf{H}_1 \mathbf{s}_1(t) + \mathbf{H}_2 \mathbf{s}_2(t) + \boldsymbol{\eta}(t), \quad (4)$$

where $\mathbf{s}_1(t) = [s(t)^T \dots s(t-\Delta)^T]^T$ indicates the symbols in the feed-forward shift register and $\mathbf{s}_2(t) = [s(t-\Delta-1)^T \dots s(t-\Delta-n)^T]^T$ denotes the symbols in the feedback register. Under the assumption that the feedback vector is correct, (4) can be re-written as

$$\mathbf{r}(t) = \mathbf{x}(t) - \mathbf{H}_2 \tilde{\mathbf{s}}_2(t) = \mathbf{H}_1 \mathbf{s}_1(t) + \boldsymbol{\eta}(t), \quad (5)$$

where $\mathbf{r}(t)$ is the observation space owing to the decision feedback. For a given feedback vector the possible noise-free channel output states in this new observation space $\bar{\mathbf{r}}(t)$ may assume $n_s = 2^{Q(\Delta+1)}$ different values, depending on the transmitted symbol vector $\mathbf{s}^{(i)}$, $1 \leq i \leq n_s$, yielding $\bar{\mathbf{r}}^{(i)} = \mathbf{H}_1 \mathbf{s}_1^{(i)}$. The set of all possible desired output states in the translated space $\bar{\mathbf{r}}(t)$ can be partitioned into two subsets \mathcal{R}_q^\pm , depending on the binary value of the transmitted symbol $s_q^{(i)}(t-\Delta)$ of the desired user q as

$$\mathcal{R}_q^\pm = \left\{ \bar{\mathbf{r}}_q^{(i,\pm)} = \mathbf{H}_1 \mathbf{s}_1^{(i)} \text{ if } s_q^{(i)}(t-\Delta) = \pm 1 \right\}. \quad (6)$$

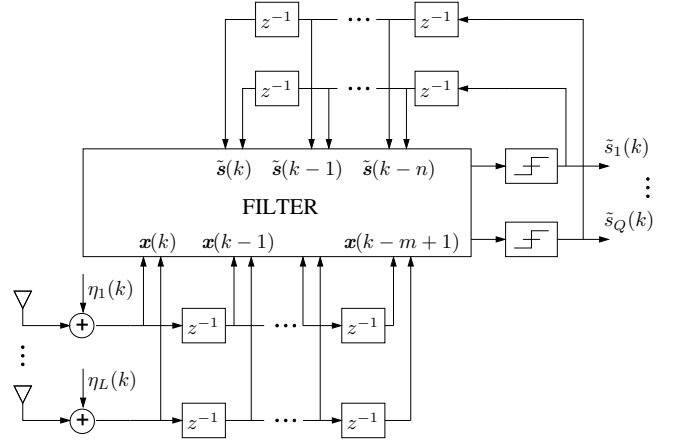


Figure 1: General structure of a decision feedback aided space-time equalizer employing L receive antennas with feed-forward order m and feedback order n . The signals $s_q(k)$ of all Q users are detected.

Based on the space translation given in (5), the decision function of the filter depicted in Figure 1 can be written as

$$\begin{aligned} \hat{s}_q(t-\Delta) &= \text{sgn}(f_{B,q}(\mathbf{r})) \\ &= \begin{cases} +1 & \text{if } f_{B,q}(\mathbf{r}(t)) \geq 0 \\ -1 & \text{if } f_{B,q}(\mathbf{r}(t)) < 0 \end{cases}, \quad (7) \end{aligned}$$

where the optimal Bayesian decision function [2] $f_{B,q}(\cdot)$ based on the difference of the associated conditional density functions is given as

$$\begin{aligned} f_{B,q}(\mathbf{r}(k)) &= P(\mathbf{x}(t) | s_q(t-\Delta) = +1) \\ &\quad - P(\mathbf{x}(t) | s_q(t-\Delta) = -1) \\ &= \sum_{\bar{\mathbf{r}}_q^{(i,+)} \in \mathcal{R}_q^+} p(\mathbf{r}(t) - \bar{\mathbf{r}}_q^{(i,+)}) \\ &\quad - \sum_{\bar{\mathbf{r}}_q^{(i,-)} \in \mathcal{R}_q^-} p(\mathbf{r}(t) - \bar{\mathbf{r}}_q^{(i,-)}) \\ &= \sum_{\bar{\mathbf{r}}_q^{(i,+)} \in \mathcal{R}_q^+} \alpha^{(i,+)} \exp\left(-\frac{\|\mathbf{r}(t) - \bar{\mathbf{r}}_q^{(i,+)}\|^2}{2\sigma^2}\right) \\ &\quad - \sum_{\bar{\mathbf{r}}_q^{(i,-)} \in \mathcal{R}_q^-} \alpha^{(i,-)} \exp\left(-\frac{\|\mathbf{r}(t) - \bar{\mathbf{r}}_q^{(i,-)}\|^2}{2\sigma^2}\right), \end{aligned}$$

where $\bar{\mathbf{r}}_q^{(i,\pm)} \in \mathcal{R}_q^{q,\pm}$, $\alpha^{(i,\pm)} = \frac{p^{(i,\pm)}}{(2\pi\sigma_n^2)^{-Lm}}$ with the a-priori probabilities $p^{(i,\pm)}$ of $\mathbf{r}_q^{(i,\pm)}$.

The Bayesian DF-STE can be realized using a RBFN employing a Gaussian kernel. The response of such a RBFN is given as

$$f_{RBF}(\mathbf{r}(k)) = \sum_{i=1}^{N_c} w_i \phi(\mathbf{r}(k), \mathbf{c}^{(i)}) \quad (8)$$

with

$$\phi(\mathbf{r}(k), \mathbf{c}^{(i)}) = \exp\left(-\frac{\|\mathbf{r}(k) - \mathbf{c}^{(i)}\|^2}{\rho}\right), \quad (9)$$

where the RBF centers $\mathbf{c}^{(i)}$ are set to the possible noise-free channel output states determined by the Channel Impulse Response (CIR), the radius ρ is chosen to be $2\sigma^2$ and the weights w_i are set to $+1$, if we have $\mathbf{c}^{(i)} \in \mathcal{R}^{q,+}$ and to -1 if $\mathbf{c}^{(i)} \in \mathcal{R}^{q,-}$. For the detection of $\tilde{s}_q(t - \Delta)$ the received signal vector $\mathbf{x}(t)$ is transformed into the translated space $\mathbf{r}(k)$ by subtracting the product of the feedback sequence $\tilde{s}_2(t)$ and \mathbf{H}_2 , given in (5). In the translated space the signal is detected using the RBFN given in (8).

3.2. Kalman Estimator

The Kalman filter based channel estimator employed was originally proposed in [4]. For the sake of deriving the estimator, the channel output vector of Equation (2) is rewritten as

$$\begin{aligned} \mathbf{x}(t) &= \mathbf{S}(t)[\text{vec}\{\mathbf{H}_0(t)\} \dots \text{vec}\{\mathbf{H}_K(t)\}]^T \\ &= \mathbf{S}(t)\mathbf{h}_{\text{vec}} \\ &= ([\mathbf{s}(t)^T \dots \mathbf{s}(t-K)^T] \otimes \mathbf{I}_L)\mathbf{h}_{\text{vec}}, \end{aligned} \quad (10)$$

where \otimes is the Kronecker product, \mathbf{I}_L is the $(L \times L)$ -dimensional identity matrix and $\text{vec}\{\}$ is the column-wise vector operator. Based on this formulation, the time-domain evolution of the vector channel \mathbf{h}_{vec} , may be expressed using an Auto-Regressive (AR) model of order p , as follows:

$$\mathbf{h}_{\text{vec}}(t) = \sum_{i=1}^p \mathbf{A}(p)\mathbf{h}_{\text{vec}}(t-i) + \mathbf{G}_0\mathbf{w}, \quad (11)$$

where \mathbf{w} is a zero-mean i.i.d circular complex Gaussian vector process. The entries of the diagonal matrices $\mathbf{A}(l)$ and \mathbf{G}_0 can be calculated using the Yule-Walker method [5] in order to match the auto-correlation of the p -th order AR model and the true auto-correlation of the channel. The parameters required for the construction of the estimator are the Doppler frequencies of the users and the delays associated with the different taps of the CIR. From the above model the Kalman filter equations can be constructed as proposed in [4].

4. CHANNEL MODEL

The channel model is based on the Power Delay Profiles (PDPs) proposed for link level simulations modeling different environments [3].

In the model used the channel between all users and all antennas is assumed to have an identical PDP. The instantaneous CIRs of the users are different due to the different complex fading experienced by the different channels. Note that the spacing of the \tilde{K} number of taps of the PDP is not necessarily an integer multiple of the symbol period T_s . Hence, in our forthcoming discourse the variables associated with the fractionally spaced PDP are therefore marked by the tilde sign. The properties of the CIRs are best explained by considering the single tap of the PDP at index \tilde{k} associated with user q , which may be written as $\tilde{\mathbf{h}}_{q,\tilde{k}} = [\tilde{h}_{1q,\tilde{k}} \dots \tilde{h}_{Lq,\tilde{k}}]$. The channel gain $E[\tilde{h}_{lq,\tilde{k}}(t)\tilde{h}_{lq,\tilde{k}}(t)^*]$ is given by the \tilde{k}^{th} tap of the PDP.

Assuming that we have a correlated Rayleigh fading channel model, the CIR may be written as

$$\tilde{\mathbf{h}}_{q,\tilde{k}}(t) = \sqrt{\text{PDP}(\tilde{k})}\mathbf{R}_{q,\tilde{k}}^{-\frac{1}{2}}\mathbf{g}_{q,\tilde{k}}(t), \quad (12)$$

where $\mathbf{g}_{q,\tilde{k}}$ is a vector of complex Gaussian coefficients having zero mean and unity variance, $\mathbf{R}_{q,\tilde{k}}$ represents the spatial covariance matrices at the receiver and $\text{PDP}(\tilde{k})$ is the \tilde{k}^{th} tap of the PDP.

Under the assumption of the underlying channel model [3] each CIR tap \tilde{k} is associated with a cluster of scatterers $\mathcal{C}_{\tilde{k}}$ of the physical propagation environment which results in a cluster of propagation paths. These path in our case result in a single, faded CIR tap since they are added up according to their phase. Each scattering cluster is characterized by the angular spread σ_{PAS}^2 of its Power Azimuth Spectrum (PAS) and the angle $\theta_{\tilde{k}}$, in which the cluster is located with respect to the perpendicular of the antenna array. Given these two parameters and the antenna spacing d spanning $\frac{\lambda}{2}$, 4λ or 10λ at the base-station antenna array, the correlation matrix can be generated using the approximate method proposed in [6].

The remaining question is now how to determine the cluster parameters. In the 3GPP-SCM [3], a number of clear strategies have been defined on how to generate the cluster parameters for given environments, which can be associated with the PDPs defined for link-level simulations. For the urban micro-cell environment of [3] for example the angular spread is fixed to 5° and the cluster angles are drawn from a uniform distribution δ spanning the range of $(-40^\circ, 40^\circ)$. For other specified environments the method is somewhat more complicated but follows the same principle.

The procedure of generating a channel matrix associated with correlated fading may be summarized as follows:

1. Generate one cluster for each of the $Q\tilde{K}$ number of CIR taps according to the procedure outlined in the 3GPP-SCM [3].
2. Calculate the $Q\tilde{K}$ number of correlation matrices as proposed in [6].
3. Correlate the uncorrelated fading coefficients $\mathbf{g}_{q,\tilde{k}}(t)$ using Equation (12).

The CIR created with the aid of the above-mentioned procedure is fractionally spaced. The DF-STE however requires a symbol-spaced CIR for its construction. Let us denote $\mathbf{h}_{lq} = [h_{lq,0} \dots h_{lq,K}]^T$ and $\tilde{\mathbf{h}}_{lq} = [\tilde{h}_{lq,0} \dots \tilde{h}_{lq,\tilde{K}}]^T$, then the symbol-spaced CIR is simply obtained with the aid of the following operation $\mathbf{h}_{lq} = \mathbf{P}\tilde{\mathbf{h}}_{lq}$, where the $(K \times \tilde{K})$ -dimensional pulse-shaping matrix \mathbf{P} is defined as

$$\mathbf{P} = \begin{pmatrix} g(-\tau_1) & \dots & g(-\tau_{\tilde{K}}) \\ g(T_s - \tau_1) & \dots & g(T_s - \tau_{\tilde{K}}) \\ \vdots & & \vdots \\ g(KT_s - \tau_1) & \dots & g(KT_s - \tau_{\tilde{K}}) \end{pmatrix}, \quad (13)$$

where $g(t)$ is the impulse response of the pulse-shaping filter. Note that the channel estimator only has to track the \tilde{K} fractionally spaced channel taps. This may be readily achieved

	Urban Micro	Urban Macro
$g(t)$	Raised Cosine	Raised Cosine
\bar{K}	4	6
K	8	14
σ_{PAS}	5°	2°
AoA	Uniform $\delta(-40^\circ, 40^\circ)$	$\mathcal{N}(0, \sigma_{AoA})$

Table 1: Simulation parameters for the generation of the correlation matrices based on the 3GPP-SCM.

by replacing $\mathbf{S}(t)$ with $\mathbf{S}(t)(\mathbf{P} \otimes \mathbf{I}_{LQ})$, where \mathbf{I}_{LQ} is the $(LQ \times LQ)$ -dimensional identity matrix.

5. RESULTS

Our initial study was carried out for two different types of Non-Line-Of-Sight (NLOS) environments, namely the urban-micro and the urban macro-cell environment [3]. The important parameters are summarized in Table 1. The system was assumed to support two users received at an equal power and employing a two-element array at the BS receiver. The normalized Doppler frequency of all users was chosen to be $f_D = 0.0005$. The DF-STE parameters were set to $m = 2$ and $\Delta = 1$. The channel estimator used 100 training symbols and tracked the channel over the 400 payload symbols in decision directed mode.

In Figure 2 the simulation results are shown for the micro-cellular urban environment using an inter-element spacing of $d = \frac{\lambda}{2}$. When comparing the MMSE-based receiver and the RBFN based receiver both benefiting from perfect channel knowledge, it can be seen that the RBFN-based receiver outperforms its linear counterpart by more than 10 dB in terms of the required SNR. Considering the effect of imperfect channel estimation, it can be observed that the first order Kalman filter exhibits tracking problems even in conjunction with correct feedback. This is due to the miss-match of the AR(1) model and the true Rayleigh fading. By contrast, the second order Kalman filter is capable of tracking the channel perfectly and is only marginally affected by error propagation.

In Figure 3 the simulation results are shown for both the micro-cellular urban and the macro-cellular urban environment for an inter-element spacing of $d = 4\lambda$ at the base-station which resulted in a CIR exhibiting richer scattering. It can be observed that the BER performance of the MMSE based receiver recorded in conjunction with perfect channel knowledge is similar for both environments. The same can be observed for the RBFN assisted DF-STE.

Comparing the graphs associated with the micro-cellular environment at an inter-element spacing of $d = 4\lambda$ in Figure 3 and the corresponding graphs in Figure 2 for $d = \frac{\lambda}{2}$, it can be seen that the performance difference between the MMSE and the RBFN based receiver became significantly smaller for the higher antenna spacing.

The effect of error-propagation on the channel estimator is also highlighted. More explicitly, the reason of error propagation is that the micro-cellular urban environment has only one dominant CIR path whereas the power of all

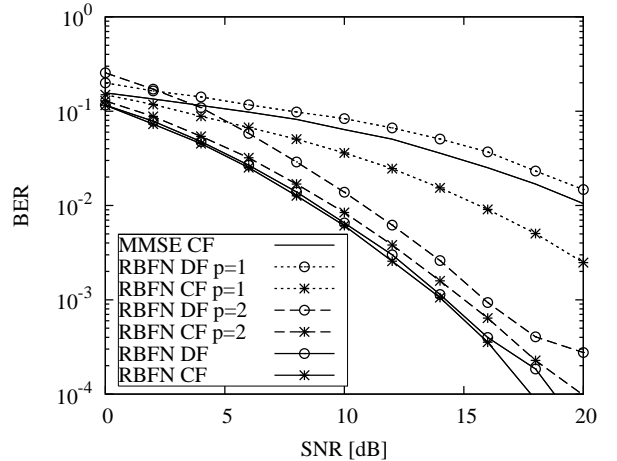


Figure 2: Average BER of a two-user beamformer versus SNR for both detected and correct feedback, when communicating in micro-cellular urban environment. A normalized Doppler frequency of $f_d = 0.0005$ was used for both users and the two users transmitted at an equal power. The receiver parameters were chosen to be $L = 2$, $m = 2$, $\Delta = 1$ and the inter-element spacing was set to $d = \frac{\lambda}{2}$. The label ‘CF’ indicates correct feedback, ‘DF’ indicates detected feedback and ‘p’ indicates the order of the Kalman channel estimator. If no order is specified, perfect CIR knowledge was assumed.

other paths is relatively low. By contrast, the macro-cellular urban environment consists of two strong paths each having almost identical power, which results in the error propagation observed.

Note that in fact the RBFN-assisted equalizer with perfect channel information reaches the single user performance for both the micro- and the macro-cellular urban environment and for different element spacings. By contrast, the MMSE BER performance observed for two users does never approach the single-user bound.

6. CONCLUSIONS AND FUTURE WORK

Our simulation results have shown that the non-linear DF-STE outperforms the linear receiver in systems supporting the same number of users as the number of antenna elements if the channel is not rich in scattering. For scattering-rich channels a significant performance difference is achieved only in over-loaded systems supporting more users than the number of antenna elements. This fact will be further highlighted in the final version of the paper along with a range of performance bounds including the single-user bound and achievable capacity in order to portray the results in a wider context.

7. REFERENCES

- [1] C. Tidestav, M. Sternad, A. Ahlen, “Reuse within a cell-interference rejection or multiuser detection?” *IEEE Transactions on Communications*, Vol.47, No.10, Oct. 1999, pp.1511-1522

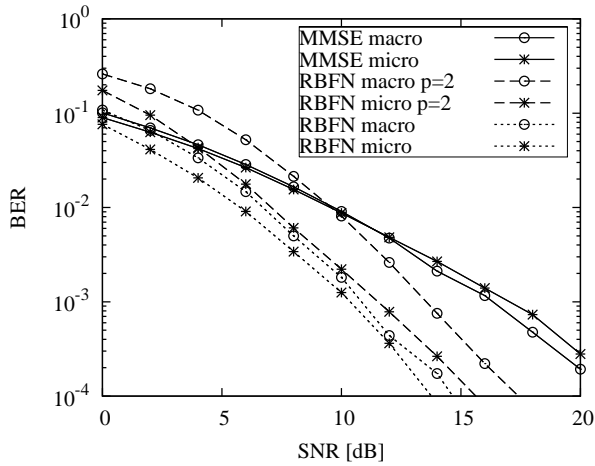


Figure 3: Average BER of a two-user beamformer versus SNR for both detected when communicating in a macro-cellular urban environment. A normalized Doppler frequency of $f_d = 0.0005$ was used for both users and the two users transmitted at an equal power. The receiver parameters were chosen to be $L = 2$, $m = 2$, $\Delta = 1$ and the inter-element spacing was set to $d = 4\lambda$. The label ‘micro’ indicates micro urban, ‘macro’ macro urban and ‘p=2’ indicates a second order Kalman channel estimator. If no order is specified, perfect CIR knowledge was assumed.

- [2] L. Hanzo, C. H. Wong, M. S. Yee: Adaptive Wireless Transceivers: Turbo-Coded, Turbo-Equalized and Space-Time Coded TDMA, CDMA, and OFDM Systems, John Wiley and IEEE Press, Feb. 2002
- [3] 3rd Generation Partnership Project (3GPP), “TR 25.996 V6.1.0, Spatial Channel Model for Multiple-Input Multiple-Output (MIMO) simulations”, 2003
- [4] C. Komninakis, C. Fragouli, A.H. Sayed, R.D. Wesel, “Multi-input multi-output fading channel tracking and equalization using Kalman estimation” *IEEE Transactions on Signal Processing*, Vol.50, No.5, May. 2002, pp.1065-1076
- [5] A. Papoulis: Probability Random Variables and Stochastic Processes, 3rd ed. New York: McGraw-Hill, 1991
- [6] A. Forenza, D.J. Love, R.W Heath Jr., “A low complexity algorithm to simulate the spatial covariance matrix for clustered MIMO channels” *Proceedings of IEEE Vehicular Technology Conference*, May 2004, CDROM